Neuro-Oncology

24(2), 229–244, 2022 | https://doi.org/10.1093/neuonc/noab175 | Advance Access date 14 July 2021

Inhibition of nicotinamide phosphoribosyltransferase (NAMPT), the rate-limiting enzyme of the nicotinamide adenine dinucleotide (NAD) salvage pathway, to target glioma heterogeneity through mitochondrial oxidative stress

Pratibha Sharma, Jihong Xu, Katie Williams, Michelle Easley, J. Brad Elder, Russell Lonser, Frederick F. Lang, Rosa Lapalombella, Deepa Sampath, and Vinay K. Puduvalli

Department of Neuro-Oncology, The University of Texas MD Anderson Cancer Center, Houston, Texas, USA (P.S., J.X., V.K.P.); Division of Neurooncology, The Ohio State University Wexner Medical Center, Columbus, Ohio, USA (P.S., J.X., V.K.P.); Department of Neurosurgery, The Ohio State University Wexner Medical Center, Columbus, Ohio, USA (M.E., J.B.E., R.L.); Division of Hematology Oncology, The Ohio State University Wexner Medical Center, Columbus, Ohio, USA (K.W., R.L., D.S.); Department of Neurosurgery, The University of Texas MD Anderson Cancer Center, Houston, Texas, USA (F.F.L.); Department of Hematopoietic Biology and Malignancy, The University of Texas MD Anderson Cancer Center, Houston, Texas, USA (D.S.)

Corresponding Author: Vinay K. Puduvalli, MD, Department of Neuro-Oncology, The University of Texas MD Anderson Cancer Center, P.O. Box 301402, Houston, TX 77230-1402, USA (vpuduval@mdanderson.org).

Abstract

Background. Tumor-specific metabolic processes essential for cell survival are promising targets to potentially circumvent intratumoral heterogeneity, a major resistance factor in gliomas. Tumor cells preferentially using nicotinamide phosphoribosyltransferase (NAMPT), the rate-limiting enzyme in the salvage pathway for synthesis of NAD, a critical cofactor for diverse biological processes including cellular redox reactions, energy metabolism, and biosynthesis. NAMPT is overexpressed in most malignancies, including gliomas, and can serve as a tumor-specific target.

Methods. Effects of pharmacological inhibition of NAMPT on cellular oxygen consumption rate, extracellular acidification, mitochondrial respiration, cell proliferation, invasion, and survival were assessed through *in vitro* and *ex vivo* studies on genetically heterogeneous glioma cell lines, glioma stem-like cells (GSCs), and mouse and human *ex vivo* organotypic glioma slice culture models.

Results. Pharmacological inhibition of the NAD salvage biosynthesis pathway using a highly specific inhibitor, KPT-9274, resulted in the reduction of NAD levels and related downstream metabolites, inhibited proliferation, and induced apoptosis *in vitro* in cell lines and *ex vivo* in human glioma tissue. These effects were mediated by mitochondrial dysfunction, DNA damage, and increased oxidative stress leading to apoptosis in GSCs independent of genotype, *IDH* status, or *MGMT* promoter methylation status. Conversely, NAMPT inhibition had minimal *in vitro* effects on normal human astrocytes (NHA) and no apparent *in vivo* toxicity in non-tumor-bearing mice.

Conclusions. Pharmacological NAMPT inhibition by KPT9274 potently targeted genetically heterogeneous gliomas by activating mitochondrial dysfunction. Our preclinical results provide a rationale for targeting the NAMPT-dependent alternative NAD biosynthesis pathway as a novel clinical strategy against gliomas.

Graphical Abstract

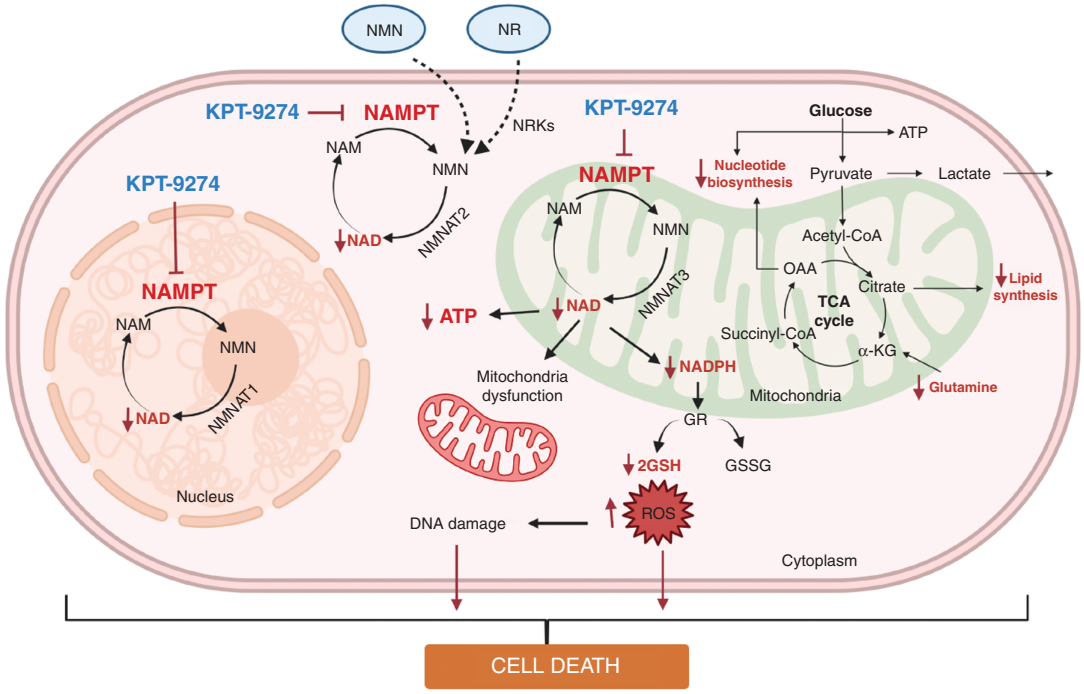

Key Points

1. Gliomas preferentially use NAMPT-mediated salvage NAD biosynthesis pathway providing a tumor-specific metabolic vulnerability.
2. Inhibition of NAMPT using KPT9274, causes mitochondrial dysfunction and cell death in gliomas independent of genetic subtype.

Importance of the Study

Gliomas are genetically heterogeneous tumors associated with a dismal prognosis due to the development of failure of standard treatments. Strategies that target individual signal transduction pathways have failed to improve clinical outcomes due to the development of adaptive resistance by the tumor cells. In contrast, targeting metabolic pathways that are preferentially used by glioma cells and not normal cells could broadly compromise multiple cellular processes in a tumor-specific manner and potentially improve outcomes. Here, we examined the feasibility of targeting NAMPT, the rate-limiting enzyme in the salvage NAD biosynthesis pathway, which is overexpressed in several cancers, in order to disable NAD-dependent enzymes that govern several cytoplasmic, nuclear, and mitochondrial metabolic processes. Pharmacological inhibition of NAMPT using KPT9274, a highly potent inhibitor, caused tumor-specific NAD depletion and widespread effects on glycolysis, lipid and nucleotide synthesis, and mitochondrial respiration, inducing cell death in gliomas independent of genetic subtype. These results provide a mechanistic rationale for the clinical development of NAMPT inhibitors against gliomas.

Malignant gliomas are lethal tumors associated with dismal outcomes and limited response to conventional therapy due to genetic and epigenetic heterogeneity.[1,2] Efforts to inhibit individual signaling pathways have been largely ineffective due to genetic and epigenetic tumor heterogeneity and the development of adaptive resistance. Additionally, the presence of glioma stem cells that exhibit radio and chemoresistance in GBM augments the heterogeneity of treatment response in these tumors, emphasizing the need for more effective therapies that target tumor-specific

pathways not influenced by heterogeneity and essential for glioma survival.[3–5]

Gliomas undergo adaptive metabolic reprogramming using pathways distinct from normal cells in order to meet their energy requirement.[6,7] One such pathway involves the biosynthesis of nicotinamide adenine dinucleotide (NAD), a critical cofactor for various cellular processes including energy metabolism, proliferation, and cell death.[8] In its metabolic role, NAD acts as a coenzyme in cellular redox reactions functioning as an electron donor or acceptor. This allows energy capture and ATP synthesis from the catabolism of nutrients such as glucose or fatty acids and supports tumor growth.[8,9] It also functions in post-translational modification reactions such as mono- or poly-ribosylation reactions essential for DNA repair and as a precursor of the second messenger molecule cyclic ADP-ribose including in cellular stress response. In addition, NAD functions as a cofactor in the protein deacetylase function of Sirtuins such as SirT1, which catalyze the removal of acetyl groups from nuclear and mitochondrial proteins and broadly influence several cellular processes.[10,11] NAD is also utilized to generate NADP, a key cofactor for anabolic cellular reactions in cells, which is crucial to maintaining cellular biomass and support proliferation. These functions emphasize the significance of the NAD in numerous cellular processes essential not only for normal cell proliferation and survival but also for malignant processes.[12]

Targeting a fundamental cellular energy generation pathway in tumor cells raises concerns that it may also affect normal tissue raising the potential for toxicity; however, unlike normal cells, malignant cells preferentially depend on the salvage pathway for the majority of their NAD synthesis providing a tumor-specific potential vulnerability that can be targeted for therapy.[13] The biosynthesis of NAD through the salvage pathway is critically governed by the rate-limiting enzyme, nicotinamide phosphoribosyltransferase (NAMPT).[8,9,14] NAMPT is highly expressed in various tumors, including gliomas, and is being explored as a promising therapeutic target for cancer treatment.[12,15–20] Its role in the malignant process has been reinforced by studies that have shown that NAMPT inhibitors such as FK866 and CHS-828 exhibit profound and selective antitumor activity leading to early clinical trials with these agents.[17,18] KPT-9274 is a potent NAMPT inhibitor demonstrating a tolerable side-effect profile and is currently in early-phase clinical trial in patients with solid tumors and lymphomas (NCT02702492).[15,19]

In this study, we demonstrate the role of NAMPT in glioma cell proliferation and survival and assess the cellular and metabolic effects of pharmacological inhibition of NAMPT using KPT-9274 in glioma cell lines, patient-derived (PDX) glioma stem-like cells (GSCs), and *ex vivo* in orthotopic mouse xenograft tissue and in human glioma tissue slice cultures.

Materials and Methods

Cell Lines and Reagents

The human glioma adherent cell lines LN229, U87, U373, T98G BT142, and A172 were obtained from the American Type Culture Collection and cultured in Dulbecco Modified Eagle Medium/Nutrient Mixture F-12 (DMEM/F12) medium supplemented with 5% FBS at 37 °C. U251-HF glioma cells were kindly provided by Dr. W. K. Alfred Yung (The University of Texas MD Anderson Cancer Center, Houston, TX). Patient-derived GSC cell lines—GSC11, GSC20, GSC23, GSC262, GSC5-22, GSC267, GSC272, and GSC811, from the lab of Dr. Frederick Lang, MD Anderson Cancer Center—were cultured as neurospheres and passaged every 3 to 5 days in serum-free DMEM/F12 medium containing B-27 supplement (Life Technologies), basic fibroblast growth factor (FGF2; Gold Biotechnology), and epidermal growth factor (Gold Biotechnology). Human Brain Microvascular Endothelial Cells are purchased from ScienCell Research Laboratories (Catalog #1000). The cells were cultured and propagated following the manufacturer's protocol. Cell lines were authenticated at the University of Arizona Genetics Core (https://uagc.arl.arizona.edu/node/27). KPT-9274, provided by Karyopharm Therapeutics Inc., was handled in the dark and prepared as a10 mM stock solution in dimethyl sulfoxide (DMSO). Smaller aliquots from this stock solution were stored at –80°C until use to avoid repeated freezing and thawing of the drug.

Construction of NAMPT Knockout Cell Lines

NAMPT knockout cells were generated as previously described by Mitchell et al.[19] Plasmids cloned with guide RNA against NAMPT promoter sequences were transfected in GSC811 and GSC5-22 cell lines stably expressing Cas9. After confirming transfection, guide RNA expression was induced by the addition of 1 μg/μL doxycycline. Induced cultures were harvested at 24, 48, 72, 96, and 120 h after induction, and NAMPT expression was determined using Western blot analysis.

Cell Viability and Cytotoxicity Assays

Water-soluble tetrazolium-1 assay.—
The adherent glioma cell lines A172, U87, LN229, U373, T98G, and U251-HF were seeded in 96-well plates at a density of 2500 cells/well. After overnight incubation, cells were exposed to vehicle (DMSO) or 0.01 to 1.0 μM of KPT-9274. Cell viability was measured at 24, 48, or 72 h after drug addition using a water-soluble tetrazolium-1 assay (Millipore Sigma) per the manufacturer's instructions.

Cell titer-glo luminescent cell viability assay—
The patient-derived GSC cell lines GSC11, GSC20, GSC23, GSC262, GSC267, GSC272, GSC811, GSC5-22, and BT142 were seeded in 96-well plates at a density of 2,500 cells/well. Cells were incubated overnight at 37°C. Next, they were treated with vehicle or 0.01μM to 1.0 μM of KPT-9274 for varying periods. Cell viability was measured using the Cell Titer-Glo Luminescent cell viability assay (Promega) per the manufacturer's instructions.

Annexin V and propidium iodide assay—
U251-HF and GSC811 cells were exposed to increasing concentrations of KPT-9274 or vehicle and incubated

for 72 h. Cells were washed with PBS and stained with Annexin V and propidium iodide (BD Biosciences) per the manufacturer's instructions. Following this, flow cytometry was performed using a BD FACSCalibur flow cytometer (BD Biosciences) with controls (unstained or stained with Annexin V or propidium iodine only) to determine the percentage of pre-apoptotic, apoptotic, necrotic, and viable cells.

Colony-Forming Assays

The LN229, U251-HF, and A172 cell lines were treated with 1.0 μM KPT-9274 or vehicle for 24 h and seeded at 1000 cells/well in triplicate in 6-well plates. After 1 to 2 weeks, colonies were fixed with 100% methanol and stained with crystal violet for 30 min. After excess stain was removed, the plates were washed and dried completely. Stained colonies were counted using Gelcount (Oxford Optronix).

NAMPT Enzyme Kinetics Assay

To assess the specificity of KPT-9274 against its target, recombinant NAMPT activity was measured using a coupled enzyme reaction (CycLex NAMPT Colorimetric Assay Kit, Cat# CY-1251; CycLex Co., Ltd.) per the manufacturer's 2-step protocol. The absorbance of the samples was detected at 450 nm at 10-min intervals for 90 min using an Infinite 200 PRO spectrometer (Tecan) and Magellan software.

Measurement of the Energy Metabolites ATP, NAD, NADH, NADP+, and NADPH

We used 96-well plates treated with Cell-Tak Cell and Tissue Adhesive (Cat# CB40240; Corning) to seed the NHA, LN229, U251-HF, GSC262, GSC811, and GSC5-22 cell lines at a density of 2500 cells/well per the manufacturer's instructions. After overnight incubation, cells were exposed to vehicle or 0.5 μM of KPT-9274 for 24, 48, and 72 h. The levels of ATP, NAD, NADH, NADP, and NADPH were quantified using Cell Titer-Glo, NAD/NADH-Glo, and NADP/NADPH-Glo assays (Promega) per the manufacturer's instructions.

Immunoblotting

Immunoblotting was performed with antibodies against SirT1 and GAPDH. DyLight-conjugated anti-rabbit and anti-mouse antibodies were used as the secondary antibodies. Details of the western blot technique and antibody sources and dilutions are provided in Supplementary Table 1.

Wound-Healing Assay

U251-HF and LN229 glioma cells were seeded in triplicate in 12-well plates at a density of 10 000 cells/well and were allowed to grow to 80% confluence. Subsequently, the cells were washed to remove floating cells. The remaining attached cells were exposed to 1.0 μM of KPT-9274 or vehicle for 24 h and a scratch was made using a large pipette tip (200 μM). Images were captured in 24 h intervals using an AxioScope A1 (Zeiss). The degree of wound-healing migration was quantitated using ImageJ software (https://imagej.nih.gov/ij/).

In Vitro Transwell Migration Assay and Microtubule Formation Assay

0.1 × 10^6 HBMEC cells were seeded in each well of 12-well plate. Once cells were attached, vehicle or 2.0 μM of KPT-9274 was added. The treated cells were grown for 64 hours then cells were detached with trypsin. Following this, cell were spin down and resuspend in fresh medium. For migration assay, equal no of viable cells from vehicle and drug-treated cells were loaded into inserts in transwell plate. For tube formation assay, cells were loaded to the wells coated with gel matrix of 24 well plate. The tube formation and migration was assessed after 6–7 h of plating and capturing photomicrographs at 10X and 20X magnifications using an AxioScope A1 (Zeiss) and quantitated using ImageJ software (https://imagej.nih.gov/ij/).

Measurement of Glioma Cell Respiration

To measure the basal respiration rate, maximum respiration capacity, and non-mitochondrial respiration of glioma cells, GSC262, GSC811, and GSC5-22 cell lines, the oxygen consumption rate (OCR), a surrogate for mitochondrial respiration, was measured using a Seahorse Bioscience XFe24 Extracellular Flux Analyzer (Seahorse XFe Analyzer; Agilent Technologies). Briefly, 4×10^4 cells were plated in an XFe24 cell-culture microplate (Agilent Technologies) treated with Corning Cell-Tak Cell and Tissue Adhesive and incubated for 60 min at 37°C to allow the cells to attach to the dish. The medium was then changed to Seahorse XF Base Medium (Cat# 102353-100; Seahorse Bioscience) supplemented with 10 mM glucose, 1 mM sodium pyruvate, and 2 mM glutamine 1h before the assay. The cells were maintained at 37°C in a carbon dioxide-free incubator. The OCR was reported in pmol/min. After the baseline measurements were made, the OCR was measured by sequentially adding 1 μM oligomycin, 0.2 5μM carbonyl cyanide-p-trifluoromethoxyphenylhydrazone, and 1.0 μM rotenone to each well.

Confocal Imaging

Per the manufacturer's instructions, 4-well Nunc Lab-Tek II Chamber Slide System slides (Cat# 154526) were treated with Corning Cell-Tak Cell and Tissue Adhesive to attach cells from the GSC262, GSC811, and GSC5-22 cell lines at a density of 25,000 cells/well. After overnight incubation, cells were exposed to vehicle or 0.5 μM of KPT-9274 for 72 h. After incubation with MitoTracker Red CMXRos (20 nM) (Cat# 9082; Cell Signaling Technologies) for 30 min, cells were fixed with 4% formalin, permeabilized with 1% Triton X, and stained with anti-Tom20 (Cat# 42406; Cell Signaling Technologies) followed by Alexa Fluor

488-conjugated anti-rabbit F(ab')2 fragment (Cat# 4412; Cell Signaling Technologies). The chambers were removed and a coverslip with a drop of ProLong Diamond Antifade Mountant with DAPI (Cat# P36962; Invitrogen) was placed on the slide. Confocal imaging was performed using an Olympus FV3000 laser-scanning microscope (Olympus).

Reactive Oxygen Species Analysis

Intracellular reactive oxygen species (ROS) levels were measured using 2′,7′-dichlorofluorescin diacetate (DCFDA; Sigma-Aldrich) via its fluorescent oxidized product, dichlorofluorescein (DCF). Briefly, cells from the GSC262, GSC811, and GSC5-22 cell lines were seeded in 6-well plates and pretreated for 6 h with 3 mM N-acetyl-L-cysteine (Sigma-Aldrich) or vehicle. After cotreatment with 1.0 μM KPT-9274 for 18 h, the cells were incubated for 60 min at 37°C in the dark with fresh complete medium containing 2 μM DCFDA. The DCF fluorescence intensity was measured using a BD FACSCalibur flow cytometer.

Measurement of Mitochondrial Membrane Potential

Changes in mitochondrial membrane potential were monitored using JC-1 dye (Sigma-Aldrich) according to the manufacturer's instructions. Cells from the GSC262, GSC811, and GSC5-22 cell lines were seeded on 6-well plates and incubated with 0.1 or 1.0 μM KPT-9274 for 72 h. The cells were then incubated with 2 μM of JC-1 for 30 min at 37°C in the dark, washed twice with cold PBS, and suspended in 500 μL of cold PBS. Fluorescence intensity was measured using a BD FACSCalibur flow cytometer. The fluorescence of J-aggregates and J-monomers was measured using excitation/emission wavelengths of 535/595 nm and 485/535 nm, respectively.

Global Metabolomics Analysis

GSC811 cells treated with 1 μM KPT-9274 or vehicle were harvested 72 h after drug treatment. The cell pellets were immediately quenched with methanol and stored frozen at –80°C. Just before analysis, the cells were thawed, spun down, and filtered using a 2 μM filtration spin tube. Samples were analyzed using a Dionex Ultimate 3000 RSLC HPLC and Agilent Zorbax SB-Aq 3 × 150 mm 3.5 μm column (Agilent Technologies) interfaced with a Thermo LTQ Orbitrap XL (Thermo Fisher Scientific) in positive polarity. Raw MS files were converted to mzXML files using ProteoWizard MSConvert (http://proteowizard.sourceforge.net/download.html) and processed using XCMS for feature detection, retention time correction, and alignment (https://xcmsonline.scripps.edu).[21,22]

Ex Vivo Effect of NAMPT Inhibition on Organotypic Glioma Slice Cultures From Mice and Humans

Organotypic slice cultures from mouse orthotopic intracranial glioma specimens or from freshly obtained human glioma specimens were prepared (Fig. 6A) as described by Xu et al.[23] and per The Ohio State University institutional review board-approved tissue collection protocol. Briefly, tumor tissue specimens were collected in pre-chilled DMEM/F-12 and GlutaMAX media (Cat# 10565018; Gibco) containing 10% FBS, kept on ice and rapidly transported to the laboratory. Tissue samples were secured in the boat of the Vibratome (Vibratome 1500 series, Vibratome) and allowed to attach for 30 seconds. The boat was then filled with pre-chilled DMEM/F-12 and GlutaMAX media and 300-μM-thick, viable glioma slices were obtained using the Vibratome. The slices were then slowly warmed to 37°C and incubated overnight. The following day, the medium was changed and the tumor slices were treated with vehicle or KPT-9274 (1 μM) for 72 h. Treated and control slices were then processed for NAD measurements and prepared for immunohistochemical analysis with hematoxylin and eosin stain, SirT1, and cleaved PARP. NAD was measured using an EnzyChrom NAD/NADH Assay Kit (Bioassay Systems) per the manufacturer's instructions.

Statistical Analysis

All *in vitro* experiments were conducted independently at least 3 times and results were expressed as the SEM. Comparisons between *in vitro* and *in vivo* groups were performed using two-tailed *t* tests. Comparisons between multiple groups were performed using a one-way ANOVA via GraphPad Prism 6 (GraphPad Software). A $P < 0.05$ was considered statistically significant.

Results

NAMPT Is Highly Expressed in Glioma Cells and Is Essential for Glioma Cell Survival

NAMPT is known to be overexpressed in several solid and hematological malignancies.[24] To assess the relative NAMPT expression level in gliomas, tissue culture lysates from normal human astrocytes (NHA), 8 adherent glioma lines: (A172, U87, U251-HF, LN229, T98G, U373, U138, and HS683), and 9 patient-derived GSCs varying in O[6]-methylguanine-DNA methyltransferase (MGMT) promoter methylation, IDH1 mutation status, and glioma subtype (GSC262, GSC811, GSC5-22, GSC23, BT142, GSC272, GSC267, and GSC20) were analyzed by Western blot. We observed a range of NAMPT expression levels, from 4-fold for GSC23 to 60-fold for U87 in comparison with NHA, indicating significant overexpression of NAMPT in GBM and GSCs and possible role in cell proliferation and survival (Figure 1A and 1B). Using an inducible clustered regularly interspaced short palindromic repeats (CRISPR) knockout of NAMPT in GSC811 and GSC5-22 cells, which caused an approximately 99% decrease in NAMPT expression 120 h after doxycycline addition, we conducted a cell viability assay comparing isogenic wild type (WT) cells and their respective NAMPT knockout versions. An approximately 50% reduction in the cell proliferation rate was noted in NAMPT knockout cells compared to WT cells, confirming the essential role of NAMPT for glioma cell proliferation (Figure 1C).

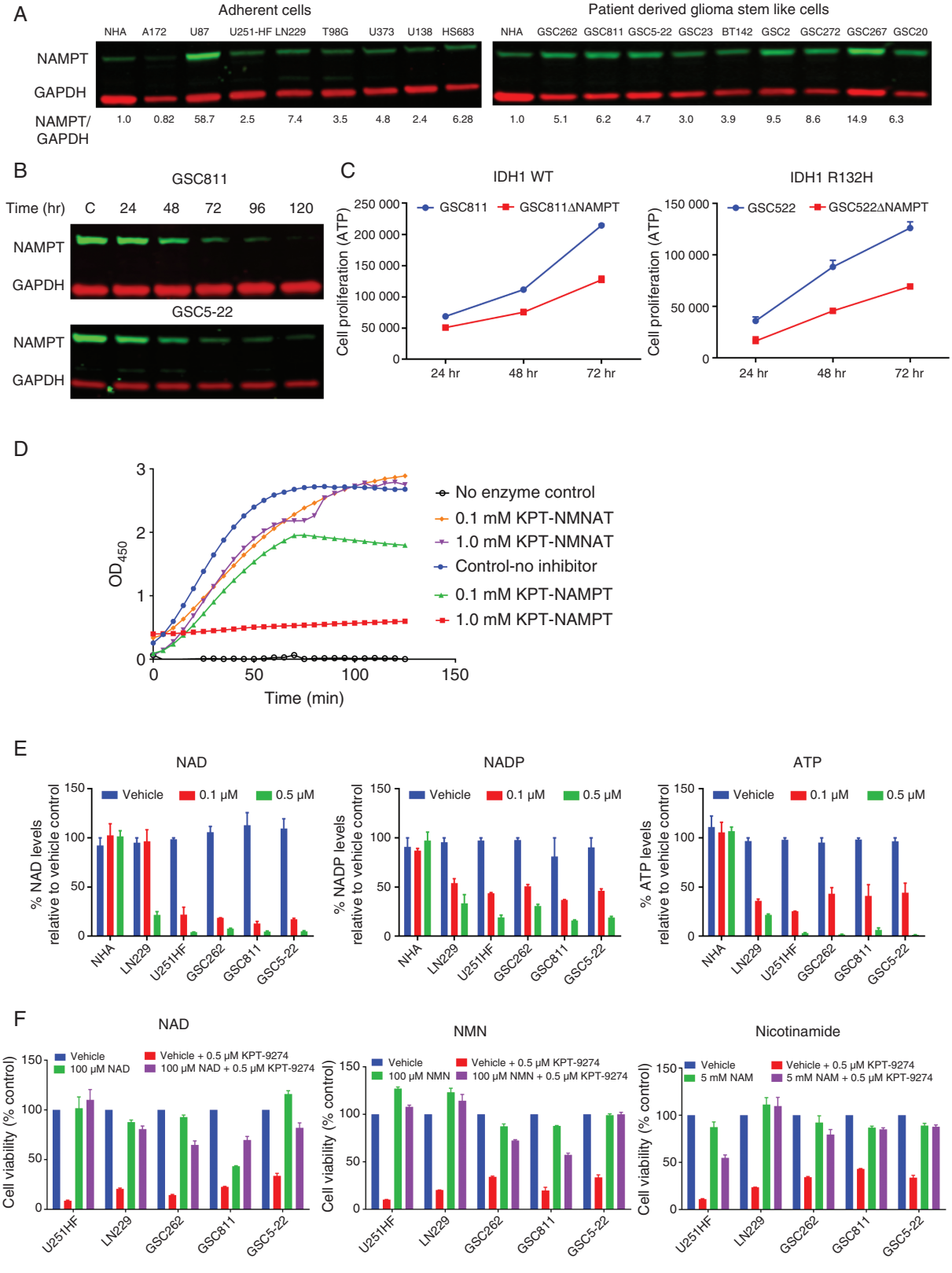

Fig. 1 NAMPT expression in gliomas and its role in cell proliferation. (A) Western blots show the NAMPT expression profiles of adherent (A172, U87, U251-HF, LN229, T98G, U373, U138, and HS683) and patient-derived glioma stem-like cell (GSC) (GSC262, GSC811, GSC5-22, GSC23, BT142,

Pharmacological Targeting of NAMPT by KPT9274 in Gliomas

To confirm the specific inhibition of NAMPT by KPT-9274, we performed an *in vitro* enzyme kinetics assay to test its inhibition against NAMPT and NMNAT. We observed that KPT9274 exhibited specific inhibition only against NAMPT enzyme, demonstrating the specificity of KPT-9274 for NAMPT (Figure 1D). To confirm that the effect of KPT-9274 was specific to gliomas and not normal cells, NHA cells as well as U251-HF, LN229, GSC262, GSC811, and GSC5-22 were exposed to 0.1 and 0.5 μM KPT-9274 and effect on energy metabolites NAD, ATP, and NADP were measured at 72 h post treatment. A dose-dependent decrease in NAD, NADP, and ATP levels was observed in both adherent glioma cells and GSCs at 0.1 and 0.5 μM; however, these energy metabolite levels remain unchanged in NHA, indicating target specificity of KPT-9274 for glioma cells and not normal glial cells (Figure 1E). Further, to assess the on-target inhibition, the adherent glioma lines U251HF and LN229, and the glioma PDX lines, GSC262, GSC811, and GSC5-22 were treated with KPT-9274 (0.5 μM) and the effect on cell viability was measured. Cells treated with KPT-9274 showed a 65–80% decrease in cell viability that could be rescued by addition of relevant NAD salvage pathway intermediates specific to NAMPT activity i.e. NMN, NAD, and nicotinamide,[8] signifying specific inhibition of NAMPT-mediated NAD salvage pathway by KPT-9274 (Figure 1F). These results further support the potential of NAMPT inhibition for treatment of gliomas.

NAMPT Inhibition Reduces the Cell Proliferation Rate and Induces Apoptosis in Glioma Cells

Glioma cells exhibit substantial intertumoral heterogeneity that can result in varied sensitivity to therapeutic agents and the development of treatment resistance.[3–5]To evaluate the effect of KPT-9274 on such heterogeneity, we measured the cell proliferation rate in glioma cells with varying genetic subtypes (proneural, classical, and mesenchymal), *MGMT* promoter methylation, and *IDH1* mutant status (Supplementary Table 2). Adherent glioma cells (A172, LN229,T98G, U251-HF) and GSCs (GSC262, GSC811, GSC5-22, BT142, GSC20, GSC272, GSC11, and GSC23) were exposed to 0.05, to 2.5 μM of KPT-9724. Based on clinically achievable concentrations in the preliminary reports of the ongoing phase I trial, cell lines which exhibited IC50 below 2 μM of KPT-9274 were considered sensitive to the agent. All tested glioma cells showed sensitivity to KPT-9274 with IC50 ranging from 0.1 to 1.0 μM at 48 h after drug addition; in contrast, NHA and HBMEC were resistant (Figure 2A and 2B). To assess the mode of cell death resulting from NAMPT inhibition, U251-HF, GSC811, and GS522 cell lines were treated with KPT-9274 or vehicle and assessed using Annexin V/propidium iodide staining. We observed a dose- and time-dependent increase in Annexin-positive cells (35%–75%), which confirmed that KPT-9274 induces apoptotic cell death in gliomas (Figure 2C). This was additionally confirmed by measuring Caspase 3/7 activity in LN229, U251-HF, GSC262, GSC811, and GSC5-22 cells after treatment with 1 μM KPT-9274 or vehicle. Cells treated with KPT-9274 showed an increase in caspase 3/7 activity compared to those treated with vehicle. We also observed an increase in caspase 8 and 9 activity, suggesting the operation of both intrinsic and extrinsic pathways for programmed cell death (Figure 2D).

NAMPT Inhibition Modifies the Biological Characteristics of Gliomas

Several processes, including angiogenesis, cellular migration, invasion, and increased cellular proliferation, define the biological behavior of gliomas.[25,26] We examined the effect of KPT-9274 on these characteristics in glioma cells and GSCs and assessed KPT-9274's effects on angiogenesis through endothelial cell tube formation assays. Treating human brain microvascular endothelial cells with KPT-9274 decreased tubule formation in a dose-dependent manner, indicating the inhibition of angiogenic potential (Figure 3A). Effect on endothelial cell invasion was tested using a transwell assay using HBMEC cells which showed a reduction of cells traversing the transwell membrane compared to vehicle (Figure 3B). A colony formation assay performed with the adherent cells, LN229, U251-HF, and A172, to examine the effect of KPT-9274 on anchorage-independent growth, showed a significant decrease in colony formation in among cells treated with 1.0 μM of KPT-9274 for 48 h compared with those treated with vehicle (Figure 3C). Additionally, cell migration, as examined by a wound-healing assay using the adherent LN229 and U251-HF cells, showed that KPT-9274-treated cells were around 50% slower in their wound-healing rate compared to vehicle-treated controls (Figure 3D).

GSCs are theorized to be the treatment-resistant stem subpopulation in gliomas that most closely exhibit the properties of human gliomas. When isolated from human gliomas, these cells are characterized by their ability to form non-adherent tumorspheres in a growth factor-supplemented, serum-free medium.[27–29] We tested the effects of KPT-9274

GSC272, GSC267, and GSC20) cell lines in comparison to the profile of normal human astrocyte (NHA). (B) Western blots illustrating the decrease in NAMPT expression in GSC811-Cas9-(NAMPT gRNA) and GSC5-22 Cas9-(NAMPT gRNA) cells caused by the addition of 1μg/μL doxycycline at 24, 48, 72, 96, and 120 h after doxycycline addition. (C) Comparison of cell proliferation between GSC811 and GSC811ΔNAMPT cells (left panel) and GSC5-22 and GSC5-22ΔNAMPT cells (right panel). (D) The results of an in vitro enzyme kinetics assay illustrate KPT-9274's specific inhibition of NAMPT enzyme activity. (E) Graphs show the targeted effect of KPT-9274 in glioma cell lines LN229, U251-HF, GSC262, GSC811, and GSC5-22, but not in NHA, as indicated by decreased levels of the energy metabolites NAD, NADP, and ATP in comparison to respective vehicle (DMSO) control. (F) Rescue of U251-HF, LN229, GSC262, GSC811, and GSC5-22 viability by addition of the NAD salvage pathway intermediates NAD, NMN, and nicotinamide. Abbreviations: NMN, nicotinamide mononucleotide; NMNAT, nicotinamide mononucleotide adenylyl transferase; OD_{450}, optical density measured at wavelength 450 nM; WT, wild type.

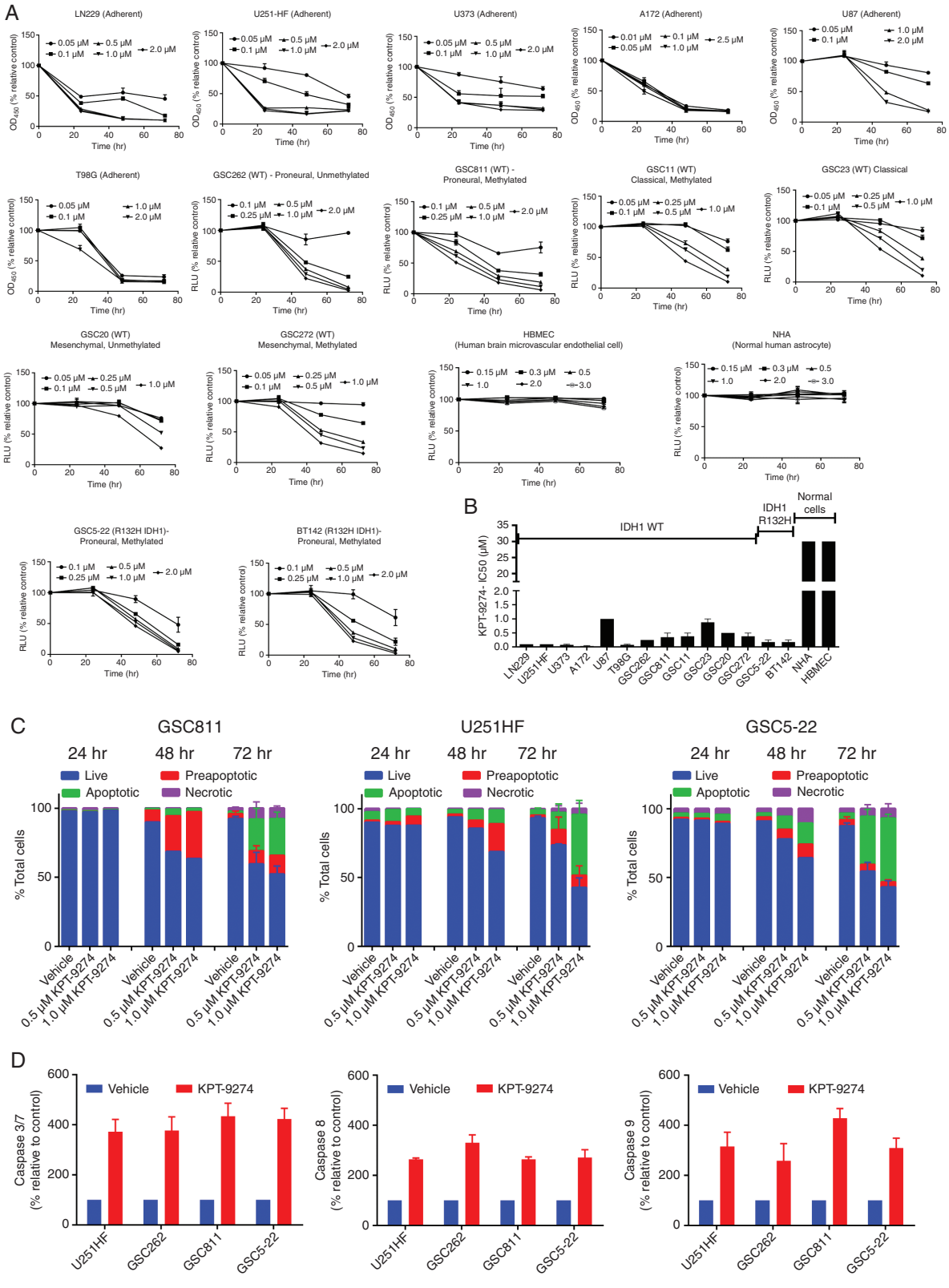

Fig. 2 The effect of KPT-9274 on glioma cell viability. (A) Cell viability assays depicting the effect of KPT-9274 on the adherent LN229, U251-HF, U373, A172, U87, and T98G cells and the patient-derived glioma stem-like cell (GSC) lines GSC262, GSC811, GSC11, GSC23, GSC20, GSC272, GSC5-22, and BT142. (B) Comparison of half-maximal inhibitory concentration (IC50) values for adherent glioma cells and GSCs. (C) The ability

on patient-derived GSCs (GSC262, GSC811, and GSC5-22) on the formation of the tumorsphere. Cells treated with KPT-9274 showed a significant decrease in sphere formation in a dose-dependent manner (Figure 3E). Further, to measure GSCs' self-renewal properties, we examined KPT-9274's effect on secondary sphere formation in these cells. GSC811 spheres were dissociated and sorted based on CD133 positivity using flow cytometry, seeded as single cells in 96-well plates, incubated overnight, and treated with vehicle or 0.06 or 0.12 μM of KPT-9274. Cells treated with KPT-9274 showed a significant decrease in secondary sphere formation properties, indicating GSCs' sensitivity to KPT-9274. A dose-dependent decrease in cell proliferation was observed in KPT-9274 treated cells as indicated by reduced luminescence by CellTiter-glo assay in drug-treated wells (Figure 3F).

NAMPT Inhibition Induces Mitochondrial Dysfunction

NAD is a key player in multiple biological processes involved in cellular metabolism and the stress response, including glycolysis and the tricarboxylic acid cycle.[8,9] NAD generation through the salvage pathway is governed by NAMPT, which is overexpressed in a variety of malignancies, including gliomas. Recent reports suggest that NAMPT inhibition may have effects on the efficiency of mitochondrial respiration.[16,19,30,31] Treatment of GSC262, GSC811 and GSC5-22 cells with KPT-9274 resulted in a decrease in levels of SirT1, a Sirtuin family member, which plays a key role in mitochondrial biogenesis and is regulated by NAMPT-mediated NAD biosynthesis (Figure 4A). To examine the effect of KPT-9274 on mitochondrial function in gliomas, GSC262, GSC811, and GSC5-22 were treated with vehicle or 0.5 μM KPT-9274 for 36 h. The oxygen consumption rate was monitored using an Agilent Seahorse assay to measure basal respiration and maximal respiratory capacity. Compared with vehicle-treated controls, KPT-9274-treated GSCs showed an approximately 85% decrease in basal respiration (Figure 4B, upper panels) and a cellular respiration capacity of only 15% of maximum, indicating functional NAMPT's essential role in cellular respiration. This defect in cellular respiration was rescued by the addition of nicotinamide mono nucleotide (NMN) a salvage pathway intermediate, confirming that the defect in cellular respiration was specifically due to NAMPT inhibition.

To further delineate the mechanism by which NAMPT inhibition caused decreased cellular respiration, we determined the overall cellular mitochondrial content of GSC cell lines using MitoTracker Red CMXRos staining and the expression levels of the outer mitochondrial protein, Tom20, using immunostaining. Although the total number of mitochondria did not change as evidenced by the expression of TOM20, a significant decrease in the number of active mitochondria was observed (as indicated by a decrease in mitotracker staining), suggesting that NAMPT inhibition by KPT-9274 caused mitochondrial dysfunction (Figure 4C). Additionally, treatment with KPT-9274 resulted in mitochondrial membrane depolarization in all 3 GSC cell lines as measured by JC-1 staining, confirming KPT-9274's direct effect in causing mitochondrial dysfunction (Figure 4D).

NAMPT Inhibition Induces Oxidative Stress and Activates the Intrinsic Apoptotic Pathway

NAD levels are closely related to the levels of several other cellular energy metabolites that act in a coordinated manner to address cellular metabolic needs. Thus, increased NAMPT expression in glioma cells increases intracellular NAD+ levels that in turn change other cellular metabolite levels. One such metabolite derived from NAD, NADP+, plays an important role in regulating the redox balance and ROS generation in cells. Cells deficient in NAMPT experience more oxidative stress and generate increased levels of ROS, which in turn can induce programmed cell death.[12,32] To delineate these changes, we first determined the alterations in cellular metabolites after NAMPT inhibition using a global metabolomics analysis of GSC811 cells treated with KPT-9274 or vehicle. Significant depletion of NAD, AMP, and deoxyguanosine monophosphate was noted, pointing to strong inhibition of the NAD salvage pathway. Additionally, KPT-9274-treated cells accumulated glucose and glucose 6-phosphate, indicating a defect in the use of available glucose and suggesting that NAMPT inhibition causes a cellular state similar to nutrient starvation (Figure 5A). We also noted decreased glutathione (GSH) levels and increased glutathione disulfide (GSSG) levels consistent with oxidative stress.[32–34] Further, accumulations of two chemicals involved in the cellular defense against oxidative stress, methionine and the glutathione precursor s-adenosyl-methionine (SAM) were noted. This stress response was also reflected in the accumulation of 8-oxo-guanine, one of the most common DNA lesions resulting from ROS and indicative of DNA damage (Figure 5A).

To further examine the effect of NAMPT inhibition on redox status in gliomas, we measured NADH and NADPH levels in LN229, U251-HF, GSC262, GSC811, and GSC5-22 cell lines treated with KPT-9274 or vehicle and found a dose-dependent decrease in both levels in KPT-9274-treated cells, indicating a redox imbalance (Figure 5B). Next, we measured the effect of this redox imbalance on ROS generation using DCFDA staining of GSC262, GSC811, and GSC5-22 cell lines treated with 1μM KPT-9274 or vehicle followed by flow cytometric analysis. We observed a 35% to 60% increase in DCFDA-stained cells, indicating ROS generation from NAMPT inhibition (Figure 5C). Because ROS generation can induce DNA damage, we

of KPT-9274 to induce apoptosis in GSC811, U251-HF, and GSC5-22 cell lines 24, 48, and 72 h after treatment as assessed by Annexin V propidium iodide flow cytometry and indicated as proportions of live, pre-apoptotic, apoptotic, and necrotic cells. (D) Measurement of caspase 3/7, caspase 8, and caspase 9 activity in the U251-HF, GSC262, GSC811, and GSC5-22 cell lines by Caspase Glo 3/7, Caspase Glo 8, and Caspase Glo 9 assays, respectively. Abbreviations: WT, wild type, $OD_{450,}$ optical density measured at wavelength 450 nM, RLU, relative light unit.

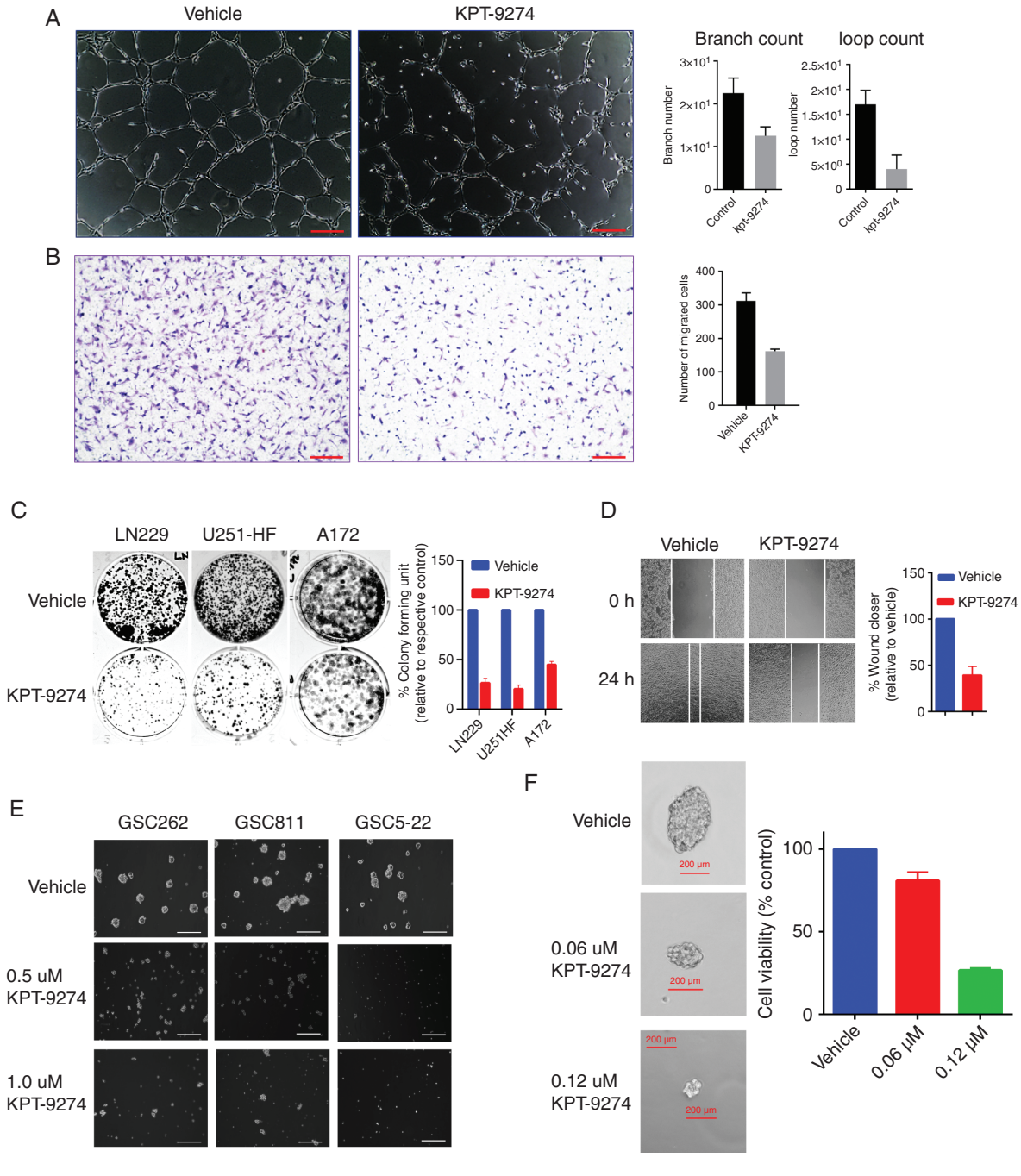

Fig. 3 The effect of KPT-9274 on the biological characteristics of gliomas. (A) The results of a tube formation assay in which human brain microvascular endothelial cells (HBMECs) were used to assess the effects of NAMPT inhibition on angiogenesis. Scale bar = 20 µm. (B) The effect of KPT-9274 on glioma invasion as assessed by a transmembrane invasion assay using HBMECs. Scale bar = 100 µm. (C) Colony formation assay using LN229, U251-HF and A172 cells. (D) Measurement of wound healing in LN229 cells exposed to KPT-9274 or the vehicle. (E) The effect of KPT-9274 on GSC262, GSC811, and GSC5-22 sphere size formation 72 h after drug exposure. Scale bar = 200 µm. (F) Dose-dependent responses to KPT-9274 of the CD133+ fraction of GSC811 cells in sphere formation and cell viability assays.

next quantified DNA damage in GSC262, GSC811, and GSC5-22 cell lines treated with vehicle or 1 µM KPT-9274 by estimating γ-H2AX levels. A 35% increase in the number of cells positive for staining indicated an increase in DNA damage from NAMPT inhibition (Figure 5D). These results confirmed that NAMPT inhibition induces mitochondrial dysfunction and consequent ROS generation, DNA damage, and apoptosis from oxidative stress.[33]

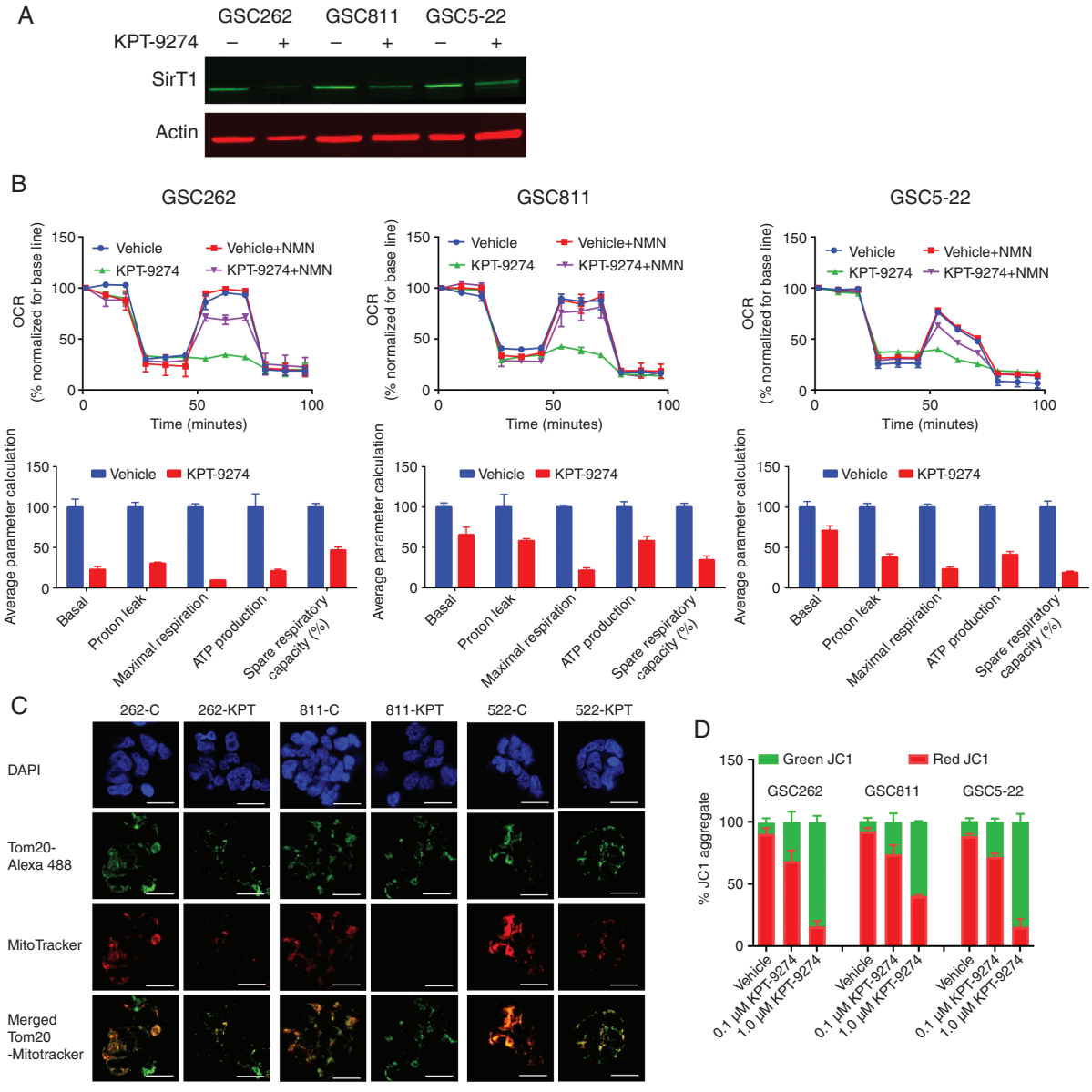

Fig. 4 The effects of NAMPT inhibition on mitochondrial function. (A) Western blot analysis of SirT1 expression in the GSC262, GSC811, and GSC5-22 cell lines. (B) Assessment of the oxygen consumption rate (OCR). An Agilent Seahorse assay was used to determine the effect of KPT-9274 on the basal respiration, maximum respiration, and spare respiratory capacity of the GSC262, GSC811, and GSC5-22 cell lines and the effect of adding 500 μM NMN, a pathway intermediate for the NAD salvage pathway, to reverse the effect of KPT-9274. (C) Immunofluorescence assays for mitochondrial morphologies, numbers, and membrane potentials in GSC262, GSC811, and GSC5-22 cells exposed to KPT-9274 or the vehicle and probed with 4′,6-diamidino-2-phenylindole (DAPI), Tom20-Alexa488, and MitoTracker Red CMXRos. Scale bar = 15 μm (D) Flow cytometric assessments of the mitochondrial potential of the GSC262, GSC811, and GSC5-22 cell lines exposed to 0.1 or 1.0 μM KPT-9274 or the vehicle and measured by staining with 2 μM JC-1 dye.

NAMPT Inhibition by KPT-9274 Depletes NAD Levels in Mouse and Human Glioma Samples

Our studies in glioma cell lines and GSCs demonstrated that NAMPT inhibition exerts potent effects in these cells by NAD depletion, which in turn leads to mitochondrial and oxidative stress resulting in apoptosis. To determine the relevance of these findings in a more translationally relevant model, we next examined whether changes in NAD levels due to pharmacological inhibition of NAMPT by KPT-9274 treatment could also be directly demonstrated in tumor tissue. Slices of viable, organotypic mouse and human glioma tissue (300 μM thick), prepared using a Vibratome, were treated with KPT-9274 or vehicle and examined for changes in NAD levels and downstream effectors. A significant decrease in NAD levels was observed

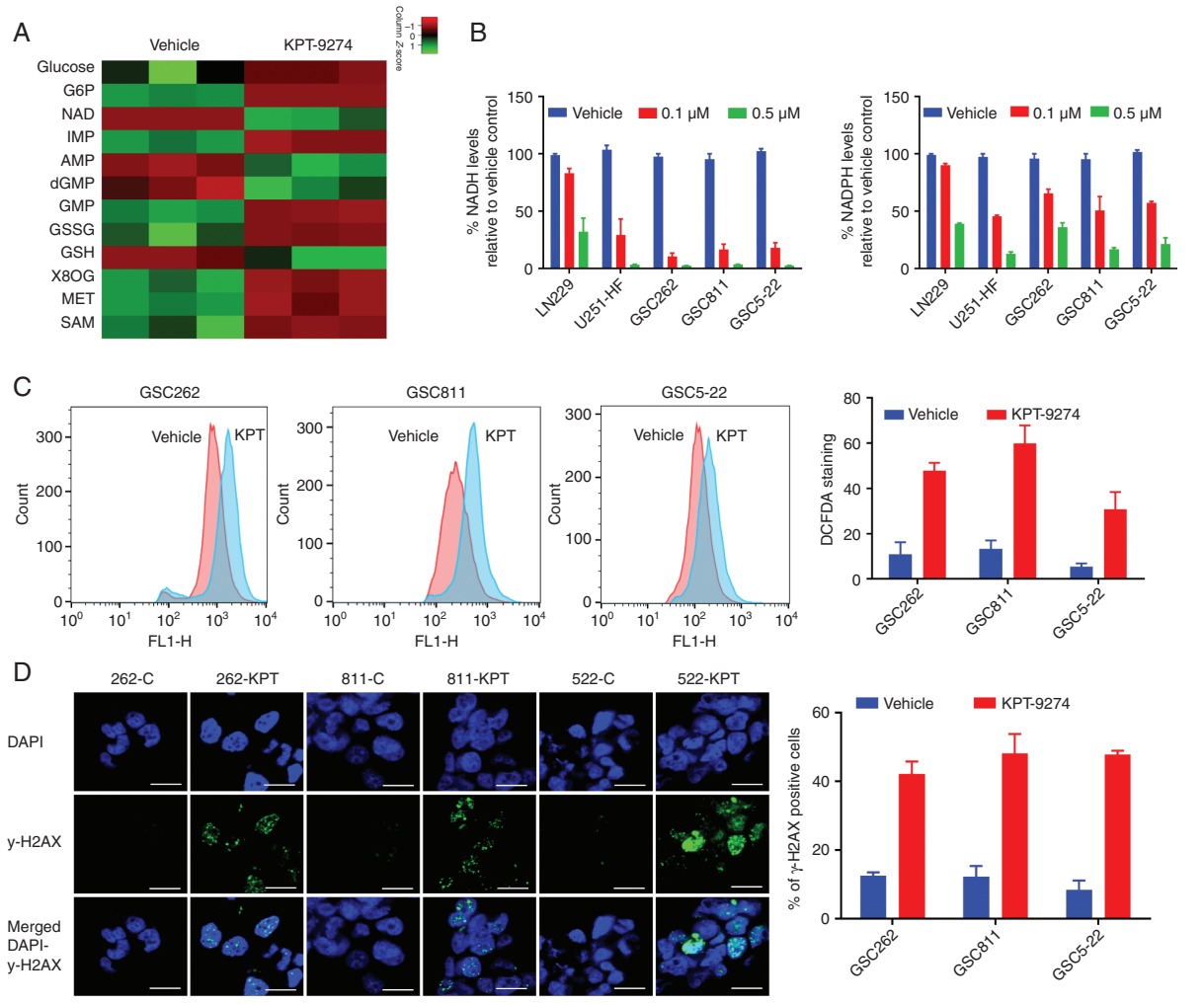

Fig. 5 The effects of KPT-9274 on cellular metabolites and oxidative stress-dependent cell death in glioma. (A) The impact of NAMPT inhibition on NAD-related cellular metabolites assessed by a global metabolomics analysis of GSC811 cells exposed to 1 μM KPT-9274 or the vehicle. The mean peak areas from technical triplicates were compared and the fold differences were plotted as a heat map. (B) The effect of KPT-9274's NAMPT inhibition on NADH and NADPH levels in LN229, U251-HF, GSC262, GSC811, and GSC5-22 cell lines. (C) The measurement of reactive oxygen species in GSC262, GSC811, and GSC5-22 cell lines by 2′,7′-dichlorofluorescin diacetate DCFDA staining. (D) Measurement of DNA damage by immunofluorescence assays for γ-H2AX and 4′,6-diamidino-2-phenylindole (DAPI) in GSC262, GSC811, and GSC5-22 cells treated with 1μM KPT-9274 or vehicle (left panel) and the proportion of γ-H2AX-positive cells after KPT-9274 or vehicle treatment (right panel) Scale bar = 10 μm. Abbreviations: G6P, glucose 6-phosphate; NAD, nicotinamide adenine nucleotide; IMP, inosine monophosphate; AMP, adenosine monophosphate; dGMP, deoxyguanosine monophosphate; GSSG, glutathione disulfide; GSH, glutathione 8OG: 8-oxo guanosine; MET, methionine; SAM, S-adenosyl methionine.

in all glioma tissue samples treated with KPT-9274 compared with those treated with vehicle (Figure 6B and 6C). Immunohistochemical analysis of the tumor organotypic tissue slices treated with KPT-9274 showed downregulation of SirT1 and upregulation of cleaved PARP levels, indicating downstream effects of NAD depletion and consequent apoptosis induction (Figure 6D). These changes in NAD and molecular markers were similar to those observed in the glioma cell lines and further support the potential of NAMPT inhibition for glioma treatment.

Discussion

Gliomas are highly resistant to conventional treatments largely due to the presence of genetically mixed cellular subtypes within each tumor, differences in regional gene expression, and the presence of multiple driver gene alterations.[35,36] Despite such heterogeneity, gliomas are critically dependent on functional metabolic processes to meet their proliferative and anabolic needs. This dependence

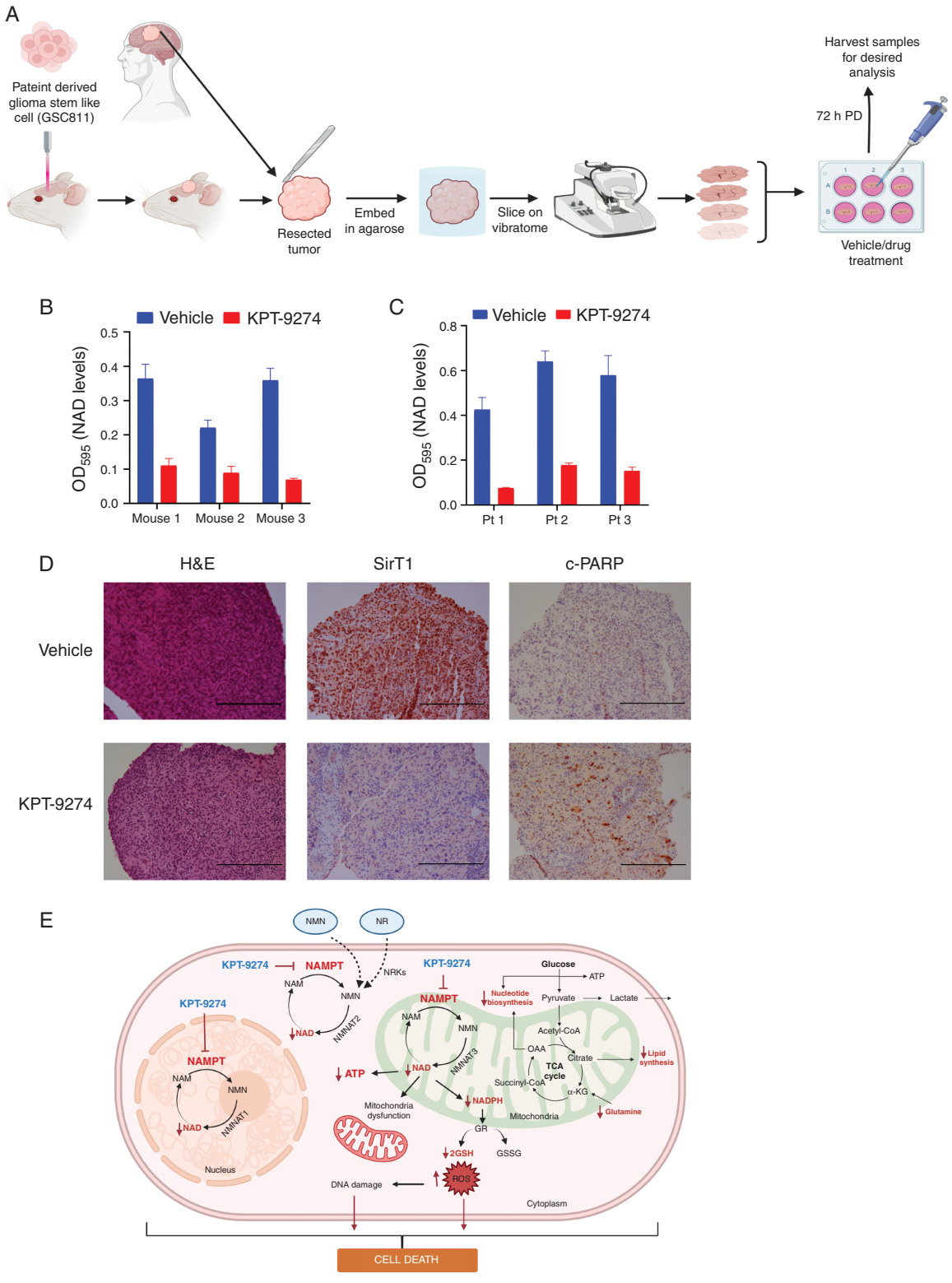

Fig. 6 The effect of NAMPT inhibition on *ex vivo* slice cultures of glioma tissue. (A) Schematic representation of method to use for organotypic slice culture experiments (B) NAD levels after KPT-9274 or vehicle treatment of mouse organotypic glioma xenograft tissue slices. (C) NAD levels after KPT-9274 or vehicle treatment of human organotypic glioblastoma tissue slices obtained during surgery. (D) Hematoxylin and eosin (H&E) stain (left panels) and SirT1 (middle panels) and cleaved PARP (right panels) immunohistochemistry specimens showing expression in vehicle- or KPT-9274-treated human organotypic glioma slice culture samples. Scale bar = 200 µm (E) Graphic depiction of the impact of NAMPT inhibition on cellular energy-dependent pathways. Abbreviation: OD_{595}, optical density measured at wavelength 595 nM.

makes gliomas potentially vulnerable to inhibitors of specific metabolic pathways. The generation of NAD and its derivative NADH, which are essential to ATP production, glycolysis, oxidative phosphorylation, DNA repair, and anabolic reactions for the synthesis of nucleotides, lipids, and proteins, is one such key requirement universally used by normal and tumor cells to sustain metabolic reactions.[37,38] However, unlike normal cells, many malignant cells overexpress NAMPT, the rate-limiting enzyme in NAD synthesis, and preferentially use the salvage pathway for NAD generation, making NAMPT an important target for anticancer therapy.[8,24,30,32,39] NAMPT is highly expressed in gliomas and is associated with a poor prognosis, further supporting the value of targeting this pathway in gliomas.[14,32,40] It has been reported that short hairpin RNA-based NAMPT downregulation affects various biological characteristics of gliomas and inhibits glioma growth *in vivo*.[41] While earlier NAMPT inhibitors such as FK866 and CHS282 have shown antitumor activity,[8,15,16,19,30,31,40,42,43] their poor bioavailability or unacceptable toxicity in human trials have precluded their development for clinical application.[17,18]

In this study, we tested pharmacological inhibition of NAMPT using KPT-9274, a NAMPT inhibitor, which has shown a tolerable safety profile and is currently in early-phase clinical trials for patients with solid tumors and lymphomas (NCT02702492).[15,19] Our finding that NAMPT is highly expressed in glioma cells and GSCs in comparison to NHAs provides a rationale for the specific targeting of this metabolic enzyme in gliomas. We also determined that NAMPT inhibition led to the depletion of NAD salvage pathway components, including NAD, NMN, and nicotinamide, in glioma cells but not in NHA, indicating that a therapeutic window for tumor-specific NAMPT inhibition exists in gliomas. Further, we demonstrated that genetic knockdown of NAMPT in both IDH WT- and IDH1-mutant glioma cells reduced the cell proliferation rate and induced apoptosis. This was further confirmed by pharmacological inhibition of NAMPT with KPT-9274, which profoundly inhibited the cell proliferation rates in multiple glioma cell lines and GSCs. Pharmacological NAMPT inhibition also induced apoptosis in both adherent glioma cells and GSCs, consistent with our genetic knockdown experiment findings and earlier reports on other cancer types.[15,19] We also observed that both the intrinsic and extrinsic apoptosis pathways were activated in KPT-9274-treated cells which, to our knowledge, has not been previously reported. Notably, these effects were independent of glioblastoma genetic subtype, IDH1 mutation status, or MGMT promoter methylation, although there was variability in the IC50 values across cell lines. Hence, our results suggest NAMPT inhibition has broad antitumor activity across glioma subtypes and contrast with the findings of a prior report suggesting that NAMPT inhibition was effective predominantly in IDH-mutant glioma cells but not in IDH WT cells.[44] This discrepancy appears to be the result of a more delayed effect of NAMPT inhibition in IDH-WT cells which does indicate higher sensitivity of IDH-mutant cells to NAMPT targeting but does not take into account that IDH-WT gliomas are also eventually susceptible to sustained NAMPT inhibition, a finding of relevance to the majority of IDH-WT GBM.

Both PAK4 and SirT1 were noted to be downstream targets of NAMPT inhibition. KPT-9274, initially described as a dual NAMPT and PAK4 inhibitor, has subsequently been shown to primarily target NAMPT through genetic studies.[20] In our study, we indeed noted the downregulation of PAK4 in gliomas, but this was a downstream effect of NAMPT inhibition by KPT-9274 and could be rescued by NAD intermediates. NAMPT inhibition causes NAD depletion that, in turn, affects the expression of several NAD-dependent genes. Of relevance to DNA damage repair, NAMPT inhibition is reported to reduce the expression of SirT1, a NAD-dependent deacetylase, that removes acetyl groups from various proteins and regulates a wide variety of biological functions, including mitochondrial biogenesis.[8,15,31,43] We noted that treatment with KPT-9274 reduces SirT1 expression levels in GSCs, an effect of NAMPT inhibition that has been observed in studies involving other cell types and various NAMPT inhibitors.[15,16,19,32] Further, we noted that NAMPT inhibition depolarizes the mitochondrial membrane and reduces mitochondrial respiration and respiratory capacity, which can critically deplete metabolic reserves in glioma cells and GSCs and make the cells vulnerable to cytotoxic stresses. Additionally, we found that NAMPT inhibition is a potent inducer of oxidative stress and causes ROS accumulation, which is known to trigger DNA damage, activate PARP, lead to ATP depletion, and ultimately cause apoptosis. Collectively, these results provide critical insights into the mechanisms of the key cellular effects of NAMPT inhibition in gliomas.

Previous studies have shown that IDH-mutant gliomas are highly sensitive to NAMPT inhibition.[44] However, this study is the first to demonstrate the antitumor activity of NAMPT inhibition across the spectrum of molecular subtypes of gliomas and to delineate the mechanistic basis of NAMPT inhibition in this tumor type. NAMPT inhibition by pharmacological means showed specific activity against glioma cells with minimal effects on NHA suggesting differences in energy utilization between normal and tumor tissue and revealing a potential therapeutic window for targeting NAMPT. In addition, NAMPT inhibition showed activity independent of glioma subtype, IDH mutation status, and MGMT promoter methylation status, which has the potential to overcome intra- and intertumoral heterogeneity, a key reason most therapies against gliomas fail. While KPT-9274 showed significant activity *in vitro* and *ex vivo*, it has limited blood-brain barrier penetrance upon systemic administration which makes clinical translation in gliomas challenging. However, we are currently exploring nano encapsulated delivery, direct intratumoral injection, and convection-enhanced delivery in preclinical *in vivo* models to overcome this limitation. Despite this limitation, our results provide strong evidence of NAMPT inhibition's translational potential as a novel energy metabolism targeting strategy against gliomas and serve as a basis for the development of other more brain penetrant NAMPT inhibitors as potential therapies for glioblastoma patients.

Supplementary Material

Supplementary material is available at *Neuro-Oncology* online.

Keywords

gliomas | KPT-9274 | metabolism | NAD | NAMPT

Acknowledgments

We thank Laura L. Russell, scientific editor, Research Medical Library, for editing this article.

Conflict of interest statement. Authors report no conflict of interest.

Authorship statement. P.S., J.X., K.W., R.L., D.S., and V.P. experimental design. P.S., J.X., K.W., M.E., B.E., R.L., F.L., R.L., D.S., and V.P. conduct of experiments. P.S., J.X., K.W., M.E., B.E., R.L., F.L., R.L., D.S., and V.P. analysis and interpretation of data. P.S. and V.P. writing of manuscript. All authors. approval of final manuscript.

Funding

This study was supported by National Cancer Institute grant K24CA160777 (for VP), the Salvino Family & Accenture Brain Cancer Research Fund, and the Ohio State University Cancer Center Support grant (NCI-CA16058).

References

1. Cloughesy TF, Cavenee WK, Mischel PS. Glioblastoma: from molecular pathology to targeted treatment. *Annu Rev Pathol.* 2014;9:1–25.
2. Stupp RMW, van den Bent MJ, Weller M, Fisher B, Taphoorn MJ, et al. Radiotherapy plus concomitant and adjuvant temozolomide for glioblastoma. *N Engl J Med.* 2005;(352):987–996.
3. Phillips HS, Kharbanda S, Chen R, et al. Molecular subclasses of high-grade glioma predict prognosis, delineate a pattern of disease progression, and resemble stages in neurogenesis. *Cancer Cell.* 2006;9(3):157–173.
4. Verhaak RG, Hoadley KA, Purdom E, et al. Integrated genomic analysis identifies clinically relevant subtypes of glioblastoma characterized by abnormalities in PDGFRA, IDH1, EGFR, and NF1. *Cancer Cell.* 2010;17(1):98–110.
5. Bao S, Wu Q, McLendon RE, et al. Glioma stem cells promote radioresistance by preferential activation of the DNA damage response. *Nature.* 2006;444(7120):756–760.
6. Strickland M, Stoll EA. Metabolic reprogramming in glioma. *Front Cell Dev Biol.* 2017;5:43.
7. Vlashi E, Lagadec C, Vergnes L, et al. Metabolic state of glioma stem cells and nontumorigenic cells. *Proc Natl Acad Sci U S A.* 2011;108(38):16062–16067.
8. Garten A, Schuster S, Penke M, Gorski T, de Giorgis T, Kiess W. Physiological and pathophysiological roles of NAMPT and NAD metabolism. *Nat Rev Endocrinol.* 2015;11(9):535–546.
9. Wang T, Zhang X, Bheda P, Revollo JR, Imai S, Wolberger C. Structure of Nampt/PBEF/visfatin, a mammalian NAD+ biosynthetic enzyme. *Nat Struct Mol Biol.* 2006;13(7):661–662.
10. Hassa PO, Haenni SS, Elser M, Hottiger MO. Nuclear ADP-ribosylation reactions in mammalian cells: where are we today and where are we going? *Microbiol Mol Biol Rev.* 2006;70(3):789–829.
11. Skidmore CJ, Davies MI, Goodwin PM, Halldorsson H, Lewis PJ, Shall S, Zia'ee AA. The involvement of poly(ADP-ribose) polymerase in the degradation of NAD caused by gamma-radiation and N-methyl-N-nitrosourea. *Eur J Biochem.* 1979;101:135–142.
12. Hong SM, Park CW, Kim SW, et al. NAMPT suppresses glucose deprivation-induced oxidative stress by increasing NADPH levels in breast cancer. *Oncogene.* 2016;35(27):3544–3554.
13. Kennedy BE, Sharif T, Martell E, et al. NAD+ salvage pathway in cancer metabolism and therapy. *Pharmacol Res.* 2016;114:274–283.
14. Gujar AD, Le S, Mao DD, et al. An NAD+-dependent transcriptional program governs self-renewal and radiation resistance in glioblastoma. *Proc Natl Acad Sci USA.* 2016;113(51):E8247–E8256.
15. Abu Aboud O, Chen CH, Senapedis W, Baloglu E, Argueta C, Weiss RH. Dual and specific inhibition of NAMPT and PAK4 By KPT-9274 decreases kidney cancer growth. *Mol Cancer Ther.* 2016;15(9):2119–2129.
16. Gehrke I, Bouchard ED, Beiggi S, et al. On-target effect of FK866, a nicotinamide phosphoribosyl transferase inhibitor, by apoptosis-mediated death in chronic lymphocytic leukemia cells. *Clin Cancer Res.* 2014;20(18):4861–4872.
17. Holen K, Saltz LB, Hollywood E, Burk K, Hanauske AR. The pharmacokinetics, toxicities, and biologic effects of FK866, a nicotinamide adenine dinucleotide biosynthesis inhibitor. *Invest New Drugs.* 2008;26(1):45–51.
18. Ravaud A, Cerny T, Terret C, et al. Phase I study and pharmacokinetic of CHS-828, a guanidino-containing compound, administered orally as a single dose every 3 weeks in solid tumours: an ECSG/EORTC study. *Eur J Cancer.* 2005;41(5):702–707.
19. Mitchell SR, Larkin K, Grieselhuber NR, et al. Selective targeting of NAMPT by KPT-9274 in acute myeloid leukemia. *Blood Adv.* 2019;3(3):242–255.
20. Neggers JE, Kwanten B, Dierckx T, et al. Target identification of small molecules using large-scale CRISPR-Cas mutagenesis scanning of essential genes. *Nat Commun.* 2018;9(1):502.
21. Adusumilli R, Mallick P. Data conversion with ProteoWizard msConvert. *Methods Mol Biol.* 2017;1550:339–368.
22. Tautenhahn R, Patti GJ, Rinehart D, Siuzdak G. XCMS Online: a web-based platform to process untargeted metabolomic data. *Anal Chem.* 2012;84(11):5035–5039.
23. Xu J, Sampath D, Lang FF, et al. Vorinostat modulates cell cycle regulatory proteins in glioma cells and human glioma slice cultures. *J Neurooncol.* 2011;105(2):241–251.
24. Lucena-Cacace A, Otero-Albiol D, Jiménez-García MP, Peinado-Serrano J, Carnero A. NAMPT overexpression induces cancer stemness and defines a novel tumor signature for glioma prognosis. *Oncotarget.* 2017;8(59):99514–99530.

25. Zagzag D, Nomura M, Friedlander DR, et al. Geldanamycin inhibits migration of glioma cells in vitro: a potential role for hypoxia-inducible factor (HIF-1alpha) in glioma cell invasion. *J Cell Physiol*. 2003;196(2):394–402.
26. Sun L, Hui AM, Su Q, et al. Neuronal and glioma-derived stem cell factor induces angiogenesis within the brain. *Cancer Cell*. 2006;9(4):287–300.
27. Kanabur P, Guo S, Simonds GR, et al. Patient-derived glioblastoma stem cells respond differentially to targeted therapies. *Oncotarget*. 2016;7(52):86406–86419.
28. Patrizii M, Bartucci M, Pine SR, Sabaawy HE. Utility of glioblastoma patient-derived orthotopic xenografts in drug discovery and personalized therapy. *Front Oncol*. 2018;8:23.
29. Tentler JJ, Tan AC, Weekes CD, et al. Patient-derived tumour xenografts as models for oncology drug development. *Nat Rev Clin Oncol*. 2012;9(6):338–350.
30. Audrito V, Manago A, La Vecchia S, et al. Nicotinamide phosphoribosyltransferase (NAMPT) as a therapeutic target in BRAF-mutated metastatic melanoma. *J Natl Cancer Inst*. 2018;110(3):290–303.
31. Imai S. Nicotinamide phosphoribosyltransferase (Nampt): a link between NAD biology, metabolism, and diseases. *Curr Pharm Des*. 2009;15(1):20–28.
32. Xu R, Yuan Z, Yang L, Li L, Li D, Lv C. Inhibition of NAMPT decreases cell growth and enhances susceptibility to oxidative stress. *Oncol Rep*. 2017;38(3):1767–1773.
33. Xiao AY, Maynard MR, Piett CG, et al. Sodium sulfide selectively induces oxidative stress, DNA damage, and mitochondrial dysfunction and radiosensitizes glioblastoma (GBM) cells. *Redox Biol*. 2019;26:101220.
34. Lozoya OA, Martinez-Reyes I, Wang T, et al. Mitochondrial nicotinamide adenine dinucleotide reduced (NADH) oxidation links the tricarboxylic acid (TCA) cycle with methionine metabolism and nuclear DNA methylation. *PLoS Biol*. 2018;16(4):e2005707.
35. Inda MM, Bonavia R, Mukasa A, et al. Tumor heterogeneity is an active process maintained by a mutant EGFR-induced cytokine circuit in glioblastoma. *Genes Dev*. 2010;24(16):1731–1745.
36. Parker NR, Khong P, Parkinson JF, Howell VM, Wheeler HR. Molecular heterogeneity in glioblastoma: potential clinical implications. *Front Oncol*. 2015;5:55.
37. Cantó C, Menzies KJ, Auwerx J. NAD(+) Metabolism and the control of energy homeostasis: a balancing act between mitochondria and the nucleus. *Cell Metab*. 2015;22(1):31–53.
38. Yang Y, Sauve AA. NAD(+) metabolism: bioenergetics, signaling and manipulation for therapy. *Biochim Biophys Acta*. 2016;1864(12):1787–1800.
39. Garten A, Petzold S, Körner A, Imai S, Kiess W. Nampt: linking NAD biology, metabolism and cancer. *Trends Endocrinol Metab*. 2009;20(3):130–138.
40. van der Veer E, Ho C, O'Neil C, et al. Extension of human cell lifespan by nicotinamide phosphoribosyltransferase. *J Biol Chem*. 2007;282(15):10841–10845.
41. Guo Q, Han N, Shi L, et al. NAMPT: a potential prognostic and therapeutic biomarker in patients with glioblastoma. *Oncol Rep*. 2019;42(3):963–972.
42. Hesari Z, Nourbakhsh M, Hosseinkhani S, et al. Down-regulation of NAMPT expression by mir-206 reduces cell survival of breast cancer cells. *Gene*. 2018;673:149–158.
43. Kim JS, Yoon CS, Park DR. NAMPT regulates mitochondria biogenesis via NAD metabolism and calcium binding proteins during skeletal muscle contraction. *J Exerc Nutrition Biochem*. 2014;18(3):259–266.
44. Tateishi K, Wakimoto H, Iafrate AJ, et al. Extreme vulnerability of IDH1 mutant cancers to NAD+ depletion. *Cancer Cell*. 2015;28(6):773–784.